MODELLING A COMPREHENSIVE RELATION BETWEEN WATER QUALITY AND CEMENT DEGRADATION IN THE DRINKING WATER DISTRIBUTION NETWORK

Karel van Laarhoven[1], Alex Hockin[2] and Martin Korevaar[3]

[1, 2, 3]KWR Water Research Institute, Nieuwegein, Utrecht, the Netherlands

[1] *karel.van.laarhoven@kwrwater.nl,* [2] *alex.hockin@kwrwater.nl,* [3] *martin.korevaar@kwrwater.nl*

Abstract

Over a quarter of the Dutch drinking water distribution network consists of cementitious pipe materials (e.g. asbestos cement, concrete and cement-coated cast iron). Leaching of cement components into the drinking water may lead to changes in water quality and to a reduction of a pipe's structural integrity. Many utilities worldwide condition their drinking water to prevent leaching. Several indices can be derived from a given water composition to estimate how well the water composition will protect against leaching. While water utilities have so far achieved good results using for instance the Langlier Saturation Index (LSI) and the Calcium Carbonate Precipitation Potential (CCPP) as an indicators, scientific authors have already posed in the past that the protection against leaching depends on a complex interplay between many chemical components in both the drinking water and the cement, and that no single index is sufficient to guarantee protection. In the presented work, a comprehensive model of the chemical and physical interactions between a cement pipe and drinking water is constructed. The model takes any given drinking water composition for input and returns a description of the chemical and microstructural changes that develop in the pipe wall over time as leaching progresses. The model shows reasonable agreement with leaching experiments described in literature. Using such a model, one can evaluate the protective capabilities of a given water quality based on all its aspects rather than just the aspects captured by derived indices. The model can be a powerful research tool for studying the interactions between drinking water and pipe materials, but this approach should also already prove to be a valuable aid for process engineers to optimize their conditioning strategies in practice, and for asset managers to translate historical water quality data to an estimation of the structural integrity of their cementitious pipes.

Keywords
Leaching, Water Quality, Asbestos Cement, PHREEQC, Transport in Porous Materials.

1 INTRODUCTION

Over a quarter of the Dutch drinking water distribution network consists of cementitious pipe materials (e.g. asbestos cement (AC), concrete and cement-coated cast iron). Given time, however, cement dissolves into wate. This process, leaching, is known as one of the most common degradation mechanisms of such pipe materials. Leaching is a problem because, first of all, it leads to components of the pipe wall entering the drinking water, changing the water quality. Additionally, leaching removes load-bearing material from the pipe wall, reducing the structural integrity of the distribution network. Leaching, therefore, must be prevented.

Many utilities worldwide condition their drinking water to prevent leaching. A key strategy is to aim at a water composition that is conducive to the precipitation of a thin layer of calcite that obstructs the contact between water and cement, thereby preventing dissolution 0. Several indices can be derived from the water composition to estimate the likelihood of such a layer forming, such as the Langlier Saturation Index (LSI) and the Calcium Carbonate Precipitation Potential (CCPP) 0, 0. While the Dutch utilities have so far achieved good results using the LSI as

an indicator, scientific authors have already posed in the past that the formation of protective layers depends on a complex interplay between many chemical components in both the drinking water and the cement, and that no single index is sufficient to guarantee protection 0, 0, 0.

The goal of the presented research is to construct and validate a numerical model of the chemical and physical interactions between a cement pipe and drinking water of any given composition. Using such a model, water utilities can evaluate the protective capabilities of a given water quality based on all its aspects, rather than just the aspects captured by derived indices such as the LSI and the CCPP. Ultimately, this should allow utilities to prevent water quality changes during distribution more effectively, and to better gauge the condition and remaining lifetime of their network.

2 MODEL

2.1 General approach

Cement is a complex composite material. It consists of several types of mineral crystals, held together by an amorphous, chemically complex gel of calcium silicate hydrates: the C-S-H gel. The crystal clusters provide a large part of the cement's structural strength. Aggregates may be added to cement to provide additional strength, such as pebbles in the case of concrete and asbestos fibres in the case of asbestos cement. Pores of different length scales are presents in the material as well, forming a microscopic network of interconnected voids that allow for some measure of fluid transport through the material.

When cement comes into contact with water, mineral crystals and C-S-H may dissolve. This makes the cement more porous and reduces the cohesion of the cement components and aggregates. This in turn reduces the overall strength of the material. Calcium hydroxide (portlandite, or CH) is one of the first minerals to dissolve and already leads to a dramatic reduction of material quality 0.

The general sequence of mechanisms that will be modelled is illustrated in figure 1. The cementitious material of the pipe is in contact with the drinking water transported by it. Due to porous transport, it is assumed that the initial pores present in the material are filled with water (1). The water in the pores equilibrates with the cement around it, so that cement components dissolve in the pore water (2). Due to concentration differences between the pore water and the drinking water outside the pipe wall, the dissolved cement components diffuse through the pore network into the drinking water (3). The flowing drinking water removes the dissolved minerals from the modelled system (4). More and more pores are formed as more and more material dissolves, making degraded parts of the material more permeable to the diffusive transport of dissolved components. This creates a positive feedback loop that has partially degraded material degrade faster and faster.

Four aspects of this general process require detailed modelling in particular: the initial cement composition; the thermodynamic stability of the different cement components, which governs how they dissolve; the diffusive transport of dissolved components through the system; and the model of the cement microstructure that governs how diffusive transport changes as the leaching progresses. These aspects are discussed in the following sections. After that, a more detailed description of the technical implementation of the model is given as well.
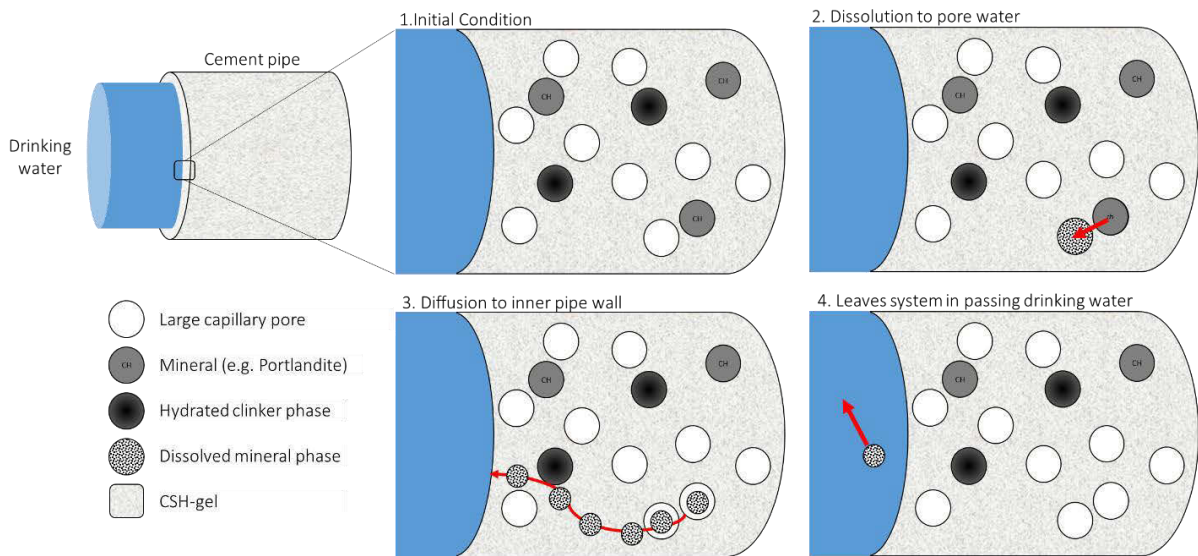
Figure 1. Schematisation of the process of cement leaching for a cement drinking water pipe. Initially, (1) cement is in contact with drinking water at the left boundary. Cement minerals and hydrated phases are present in the cement. (2) Cement components dissolve into the water present in the pores, leaving additional pores behind. (3) The dissolved mineral diffuses from the inner cement through the pipe wall towards the drinking water. (4) The dissolved mineral is removed from the system by the passing drinking water.

2.2 The thermodynamic stability of cement minerals

The dissolution or precipitation of minerals in cement is determined by the mineral thermodynamics. Minerals precipitate or dissolve to achieve chemical equilibrium in the system. When a system is in equilibrium, the Gibbs free energy of the system is at a minimum and all chemical reactions are in equilibrium. Mass action equations relate changes in the Gibbs free energy of reaction the mass action constants 0. In chemical equilibrium modelling, the mass action equations and conservation of mass are used to calculate the equilibrium state of a system 0. In order to calculate the chemical equilibrium of a system, chemical modelling software is used 0. This work uses one example of such software: PHREEQC.

PHREEQC requires a database that contains data (aqueous speciation and activity coefficients) of the elements in the modelled system, to evaluate their equilibrium. A specialized cement database (CEMDATA07), compiled by Lothenbach et al., 0, 0 and converted for use in PHREEQC by Jaques, 0, is used for the purposes of this model. This database compiles mass action constants for cement minerals from literature and practice. Importantly, the database also implements a model to represent the complex C-S-H gel as a system of a reduced number of specific hydrates: tobermorite-II ($Ca_5Si_6O_{16}(OH)_2 \cdot 4H_2O$), jenite ($Ca_9Si_6O_{18}(OH)_6 \cdot 8H_2O$) and amorphous silicagel (SiO_2). Tabel 1 summarizes the different phases that are selected as relevant components of cement for PHREEQC to evaluate in the model.

Table 1. Mineral phases and elements in the model.

Mineral	Description
CALCIUM-SILICATE-HYDRATES (CSH)	The C-S-H gel is modelled as an ideal solid solution of Jennite ($Ca_9Si_6O_{18}(OH)_6 \cdot 8H_2O$), tobermorite-II ($Ca_5Si_6O_{16}(OH)_2 \cdot 4H_2O$) and a pure phase of amorpheous silciumdioxide (SiO_2).
AFT-PHASES	An ideal solid solution of ettringite-tricarboaluminate is present as the most important Aft-phase.

OTHER PHASES	Other cement minerals that are included are: hydrotalcite, calcite, portlandite, monocarboaluminate, stratlingite, hydrotaliceOH. Included elements are: Al, C, Ca, K, Mg, Na, S, Si. Iron was not included in the model as Jacques et al., 0, found it led to unnecessarily complicated calculations and its inclusion had no effect on the evolution of pH, element concentrations and solid phase composition.

2.3 The chemical composition of the cement

Ordinary Portland Cement (OPC) was chosen as the default cement composition for the model, as this is the type of cement used in the majority of Dutch asbestos cement pipes 0. OPC consists of four major clinker phases: alite (C3S), belite(C2S), aluminate (C3A) and ferrite (C4AF) 0. The exact composition of elements used as a default is CEM I 42.5, as reported in Table 2, but can be modified to match other types of cement if so desired. When a defined amount of water is added, these clinker phases slowly hydrate to form the various cement hydrates.

The initial composition of the hydrated cement is obtained during the initialization of the model by entering the OPC composition from table 2 in PHREEQC as a solution of the components in a certain amount of water. The amount of water is chosen according to a desired 'water to cement mass ratio' (w/c). PHREEQC then converts this solution to the corresponding composition of hydrated mineral crystals and C-S-H gel present in table 1, assuming complete hydration (α) of the clinker products. In fully hydrated cement ($\alpha=1$), all cement clinker has reacted and no unreacted clinker is left. Under regular mixing conditions, the degree of hydration is less than 1 and can be calculated from empirical formulas from literature (e.g. 0). The main producer of Dutch AC pipes, however, reports that their material is produced under circumstances (high pressure and humidity) that are conducive to full hydration 0. Note that a w/c of at least more than approximately 0.27 is required to provide sufficient water molecules for complete hydration (higher w/c may influence the specific composition of hydrated components and the microstructure of the cement, as discussed below).

Table 2. CEM I compositions of Ordinary Portland Cement according to 0.

	CEM I 42.5 N 0	**CEM I 52.2 N 0**
Mineral	**g/100 g OPC**	**g/100 g OPC**
CaO	62.4	67.4
SiO_2	18.9	23.4
Al_2O_3	4.4	30.5
Fe_2O_3	2.5	2.15
CaO (free)	0.6	-
MgO	1.4	0.7
K_2O	0.95	0.15
Na_2O	0.10	0.1

CO_2	2.1	-
SO_3	3.0	2.1

2.4 Microstructure model of degrading cement

The porosity of the cement plays a key role in the diffusive transport of solutes (as will be discussed below). The porous structure of the cement must therefore be addressed in the model, especially since the leaching of cement will result in progressive changes in the porous structure. The well-established cement models of Powers et al., 0, as reviewed by Brouwers, 0, are used to estimate the initial volume fractions of the cement and its pores. As discussed, the cement consists of minerals (e.g. portlandite, calcite etc.) and a CSH-gel. The porous structure of the cement contains roughly two types of pores with different length scales: 'capillary pores' (0.1-1 µm), which are voids between the crystals and gel; and the smaller 'gel pores' (5-50 nm), which are voids between the molecules that constitute the C-S-H gel.

The capillary porosity depends on the circumstances under which cement is produced: it is a function of the water to cement ratio and the degree of hydration 0. With increasing *w/c* and decreasing α, the initial capillary porosity of cement increases. This is because water consumed by hydration becomes part of the cement material, but the water in excess of the amount consumed by hydration remains distributed across the curing cement, resulting in the formation of capillary pores 0. Powers et al., 0, provide empirical formulas for the individual volume fractions of the capillary pores, θ_{cp}, and the gel pores θ_g, that arise in cement under regular mixing conditions:

$$\theta_{cp} = \frac{w/c - 0.36\alpha}{w/c + 0.32} \tag{1}$$

$$\theta_g = \frac{wc - 0.17\alpha}{wc + 0.32} - \theta_{cp} \tag{2}$$

As mentioned above, the cement in AC pipes was not produced under regular mixing conditions, but under circumstances (high pressure and humidity) that are conducive to full hydration at very low w/c, so that very few capillary pores are formed 0. Because of this, (1) and (2) are likely not suitable to use directly for AC. To determine the initial microstructure of AC specifically, first regular cement was simulated with PREEQC (assuming a *w/c* of 0.4-0.5 and an α of 1). Evaluating (1) and (2) for this cement, it follows that e gel pore volume is approximately equal to 70%-95% of the volume of the C-S-H minerals. Subsequently, it is assumed that the AC production process negates the creation of capillary pores but leaves the voids in the C-S-H gel unchanged. The total volume and porosity of the AC is then recalculated from: the volume of the hydrated products, the volume of the gel pores, and the volume of an added amount of asbestos aggregate.

In cement-aggregate systems, such as concrete or asbestos cement, the porosity of the cement close to the aggregate may be modified. This leads to a interfacial transition zone (ITZ), a zone of heightened porosity and permeability, between the bulk cement paste and aggregate particles like pebbles or asbestos fibers 0. This zone is important in composite systems, because it may substantially facilitate diffusive transport. Focussing on asbestos cement, however, the importance of the ITZ is negligible because the asbestos fibers are not thick enough to influence the porosity of the surrounding cement 0. The ITZ is therefore not considered in this study, but may need to be included when studying for instance concrete pipes.

To evaluate how the microstructure changes during leaching, it is assumed that the dissolution of a certain volume of cement components results in the creation of an equal volume of capillary

pores. When C-S-H components dissolve, however, also a proportional volume of gel pores is converted to capillary pore volume. As capillary pores are far larger than gel pores, they would form the main transport path for diffusion. If the production circumstances lead to a low capillary porosity, however, capillary pores may not form a connected network, whereas gel pores are ubiquitous as they are linked to the C-S-H gel. Diffusion through gel pores therefore also contributes and even dominates transport at very low capillary porosity 0. A critical capillary porosity (θ_{ccp}) may be identified below which there is no transport through the capillary pores (Figure 2).

$\emptyset_{\text{capillaire}} < \emptyset_{\text{critical}}$ $\emptyset_{\text{capillaire}} > \emptyset_{\text{critical}}$
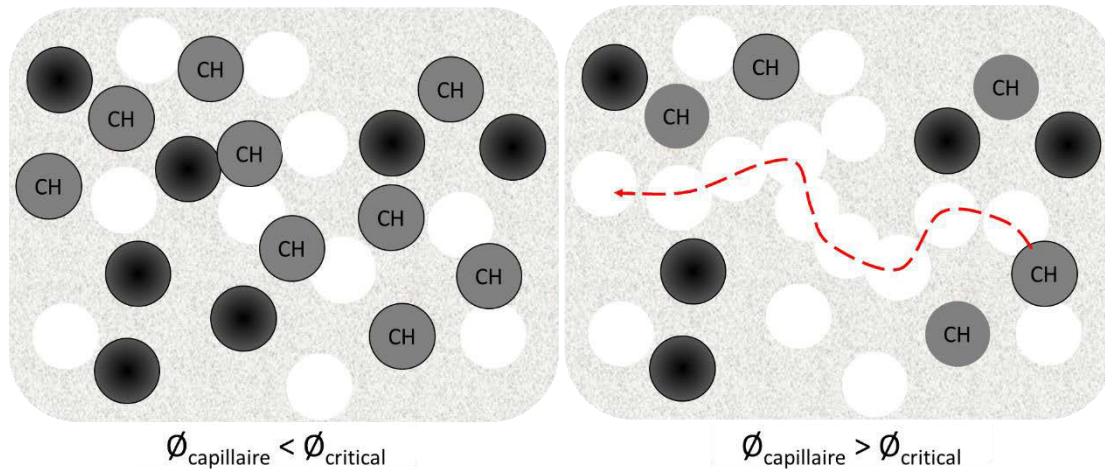
Figure 2. Visualization of the connectivity of the capillary pores (open circles). Grey and black cicles represent the cement minerals and the light grey background represents the porous CSH-gel. Left: below the critical capillary porosity, capillary pores are disconnected and diffusion (red line) through capillary pores does not occur. Right: above the critical capillary porosity, capillary pores are connected and diffusion through capillary pores occurs.

2.5 Diffusive transport of dissolved minerals through the degrading porous material

Diffusion is the resulting movement of particles from regions of higher to lower concentration, as described by Fick's Law 0:

$$F = -D \frac{\partial c}{\partial x} \tag{3}$$

Where F is the flux [mol/s/m^2], D is the diffusion coefficient [m^2/s] and c is the concentration [mol/m^3]. The diffusion coefficient depends on, among other things, the ion size, the temperature and interaction with other diffusing species due to species charge. Oppositely charge species can accelerate while similarly charged species can retard diffusion 0. Detailed data on the diffusion coefficients for elements is not always available, therefore for multi-component diffusion an average diffusion coefficient in free water is currently used 0. Diffusion of elements in porous systems must travel longer distances than in bulk water. The TRANSPORT block of PHREEQC accounts for this with a hardcoded relation for an effective diffusivity, D_e:

$$D_e = [\theta]^n D_0 \tag{4}$$

Where θ is the total (water-filled) porosity [-] and n is the Archie's constant [-]. As described in the previous section, however, not only the overall porosity of the cement changes during leaching, but also the connectivity between (capillary) pores changes. To account for this, a more suitable effective diffusion coefficient is instead taken to be D_{GEM}, obtained with the general effective medium (GEM) equation reported by Oh et al., 0:

$$D_{GEM} = [\theta_{GEM}]^n D \tag{5}$$

$$\theta_{GEM} = m_\theta + \sqrt{m_\theta^2 + \frac{\theta_{ccp}}{1 - \theta_{ccp}}\left(\frac{D_s}{D_0}\right)^{\frac{1}{n}}} \tag{6}$$

$$m_\theta = \frac{1}{2}\left[\left(\frac{D_s}{D_0}\right)^{\frac{1}{n}} + \frac{\theta_{ccp}}{1 - \theta_c}\left(1 - \left(\frac{D_s}{D_0}\right)^{\frac{1}{n}}\right) - \frac{\theta_{ccp}}{1 - \theta_{ccp}}\right] \tag{7}$$

Where θ_c is the capillary porosity, D_s/D_0 is the normalized diffusivity through solid C-S-H (when the capillary porosity is zero), D_0 and D_s are the diffusivities [m²/s] in, respectively, bulk water (i.e. the maximum effective diffusivity possible), and in the solid C-S-H (i.e. the minimum effective diffusivity possible). For Portland cement pastes, $n \approx 2.7$ and $D_s/D_0 \approx 2.0*10^{-4}$ 0. The critical capillary porosity is approximately 0.18 0. Inserting θ_{GEM} into (3) provides PHREEQC's transport module with a suitable, leaching-dependent diffusivity for cement.

2.6 Technical implementation of the model

The concepts in the sections above were combined into a numerical model using the geochemical code of PHREEQC 3.3.7, 0, through the python package PhreeqPython 0. CEMDATA07 was used as the chemical database for PHREEQC. The model is set up and initialized as follows:

1. A representative volume of (asbestos) cement is initialized by creating a solution of an amount of clinker (e.g. with the composition in table 2) in an amount of water according to a chosen w/c and evaluating it with PHREEQC (resulting in a composition of the components listed in table 1). The initial composition of the pore water is taken to be the composition that is in equilibrium with the initialized cement.

2. The diffusive transport is implemented as 1D diffusive transport using the TRANSPORT keyword in PHREEQC. Electro-diffusive phenomena are neglected. Consequently each aqueous species has the same diffusion coefficient 0. Using the multi-component diffusion option in PHREEQC, overall charge balance is maintained 0.

3. For the purposes of transport, the volume of cement is discretized in a number of cells of thickness l with a combined thickness L in the direction of transport.

4. One boundary condition is set as closed on one side (Neumann type boundary condition), representing the external wall surface of the cement pipe (which is not in contact with the drinking water). The other boundary condition (inner pipe wall) is set as a constant set of concentrations, representing exposure to any (continuously refreshed) drinking water composition (Dirichlet type boundary condition).

5. The initial capillary porosity and gel porosity are determined from the initialized cement as described in paragraph 2.4, with equations (1) and (2) and specific assumptions in the case AC is being modelled.

Simulation of the leaching in this system is then achieved by the following cycle for each numerical timestep:

1. For each cell, the effective porosity θ_{GEM} is determined with equation (6), based on each cell's current θ_{cp}.

2. The θ_{GEM} is implemented in the transport block using the built-in BASIC command program of PHREEQC. To save computational time, the GEM porosity may be updated less

frequently. No difference was observed with performing the calculation after each time step versus after every 100th time step.

3. Diffusive transport (mediated by the θ_{GEM}) between the pore water solutions of neighbouring cells (and the drinking water boundary condition) is evaluated with PHREEQC.

4. Equilibration between the cement in each cell and its new pore water composition is evaluated with PHREEQC.

5. Based on possible precipitation or dissolution of components in a cell during step 4, the θ_{cp} of each cell is updated.

3   PRELIMINARY OUTCOMES AND DISCUSSION

3.1 Example results and grid sensitivity

The raw output of the model consists of the chemical composition of the cement and pore water in each cell, and the derived porosities, for each timestep. Figure 3 display examples of data from a series of simulations performed for the purposes of a grid sensitivity study of the model. The initial cement composition from 0 in table 2 was used (and was not modified to resemble AC as discussed in paragraph 2.4). Other model parameter values, as mentioned earlier, were: w/c = 0.5; D_S/D_0 = 2.0*10^{-4}; α = 1, θ_{ccp} = 0.18, n = 2.7. Pure water was used for the water composition at the Dirichlet boundary condition. A system length L of 5 mm was chosen. A simulation of 114 days of leaching in this system was repeated for different discretization length scales (l = 1, 0.5, 0.25, 0.125, 0.0625).

Figure 3 shows two profiles of aspects across the system after the simulation: the number of moles of portlandite remaining in each cell and the pH of the pore water in each cell. With respect to the different l, it can be seen that succeeding solutions become more similar with decreasing l, and that further reduction of l below 0.125 do not lead to substantial changes in the profiles. Moreover, it can be seen that – as is expected to occur during leaching – a sharp leaching front in terms of portlandite depletion forms during leaching, but that in the degraded part of the cement does have variation in its chemical composition, as can be gleaned from the different pHs in the degraded cells.

3.2 Verification from literature

The model was verified by using it to emulate a number of laboratory leaching experiments and comparing the outcomes. Moranville et al., 0, reported leaching experiments of 114 days with cement of different w/c (0.25, 0.4, 0.5), exposed to different water qualities (pure water and mineral water with the composition reported in table 3). The composition of their cement differs slightly from the CEM I previously discussed and is included in table 2. The model was used to reproduce these conditions, further using a grid size of l = 0.1 mm. Moranville reported the overall porosities of their samples, and the initialized cement was modified by adjusting the θ_{cp} of the initialized cement to match this. Moranville defined the results of the experiments in terms of the, visually observed, depth of portlandite leaching after the 114 days.

Table 3. mineral water composition (pH = 7) used in the experiments reported in 0.

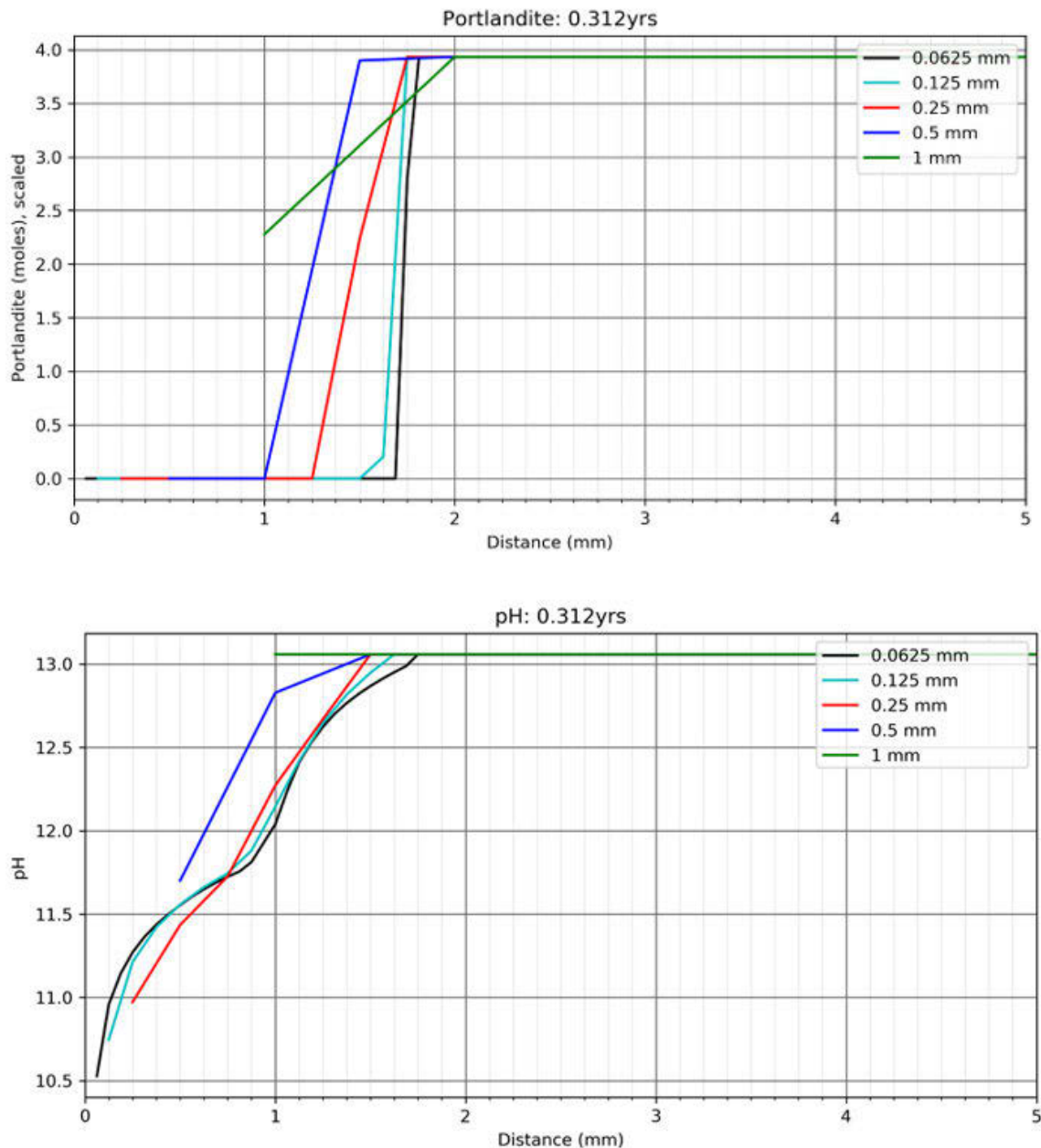| Element	Ca	Si	Mg	Na	K	Cl	SO$_3$	HCO$_3$
Concentration [mg/L]	11.5	31.7	8	11.6	6.2	13.5	8.1	71

Figure 3. *Outcomes of grid independence simulations of 114 days of 1D leaching of Portland cement exposed to pure water at distance 0. Shown are profiles across the system of portlandite content (upper) and pore water pH (lower). With decreasing grid size, the depletion front for portlandite become sharper and the change in pH between cells smoother.*

Figure 4 compares the results of Moranville with the model outcomes. The progression of the portlandite front over time for the model simulations is shown by the green curves, and the snapshot measurements reported by Moranville are shown by the black markers. The model results follow the same trend as the lab results. The lower *w/c* leads to a reduced initial capillary porosity, which in turn leads to slower leaching. On top of that, exposure to mineral water results in even slower leaching; presumably due to slower dissolution and diffusion of cement components in the pores and due to deposition of calcite scaling obstructing diffusion even further.
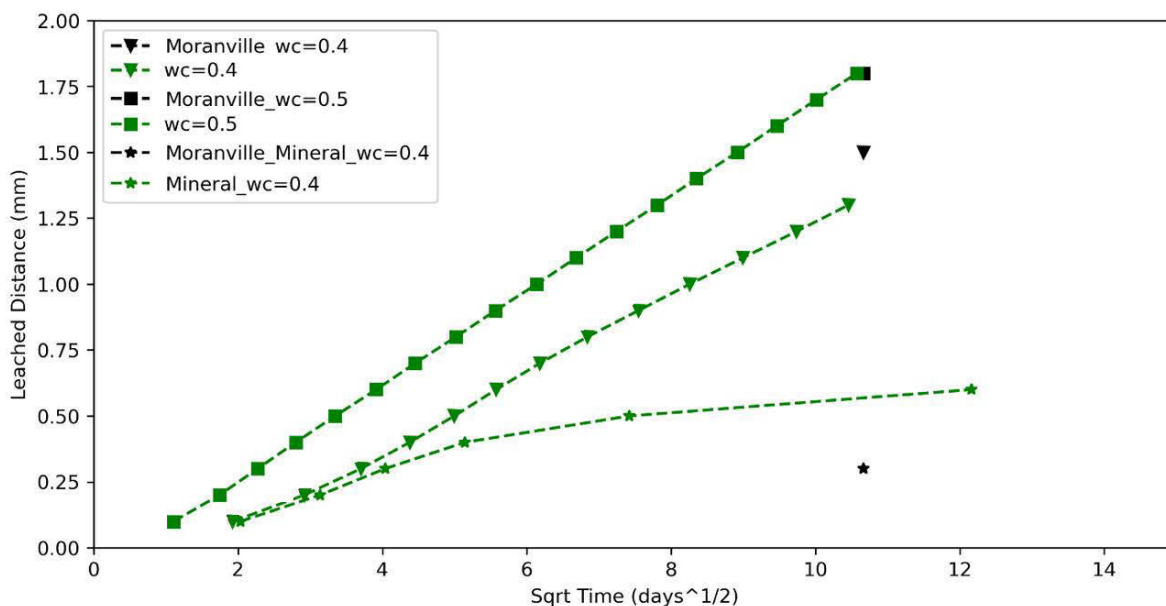
Figure 4. Comparison of the model outcomes to the experiments reported by 0. Green curves indicate the modelled progression over time of the leached dept. Black markers indicate the reported leached depths at the end of the experiments. The different symbols indicate which scenario was modelled: w/c = 0.5, exposed to pure water (squares); w/c = 0.4, exposed to pure water (triangles); and w/c = 0.4 exposed to the mineral solution summarized in table 3 (stars).

Carde et al., 0, reported a different set of leaching experiments, in which cement was exposed to demineralized water of pH = 4.5 and the leaching depth was measured after 90 and after 210 days. Carde used the CEM I 42.5 cement reported in table 2, with a *w/c* of 0.5, but with no measured porosities reported. The porosities of the cement were therefore estimated with equations (1) and (2). Because preliminary tests with the model showed a substantial sensitivity of results to the initial porosity, and additional simulation with *w/c* = 0.55 was carried out. The initial capillary porosities for *w/c* 0.5 and 0.55 are, respectively, 17 and 21.8 %.

Figure 5 shows the leached depth reported in Carde (black) and in the simulations with w/c =0.5 (blue) and w/c=0.55 (red). The results shows reasonable agreement with both simulations, with closer results for the simulations with the high w/c ratio (w/c = 0.55). Indeed, the model is sensitive to the initial capillary porosity, therefore without reported porosities to validate the initial porosity it is more difficult to get a very good fit, and the estimations of porosities with the empirical equations of Powers may not be completely suitable. However, even the simulations with the w/c of 0.5 (reported value in 0) the simulations are within 0.2 and 0.3 mm of the leaching after 90 and 210 days respectively. This is improved to 0.1 mm in the simulation with w/c = 0.55 for both the leached depth after 90 and 210 days.

4   CONCLUSIONS AND OUTLOOK

A numeric model for simulating the leaching and scaling processes in cementitious pipe materials exposed to a specific drinking water quality was presented. This model can be a powerful research tool for studying the interactions between drinking water and pipe materials, but this approach should already also prove to be a valuable aid for process engineers to optimize their conditioning strategies in practice, and for asset managers to translate historical water quality data to an estimation of the remaining structural integrity of their cementitious pipes.

At the moment of writing, steps are being taken to further refine different aspects of the model, such as bringing it in line with the most recent version of the CEMDATA database (CEMDATA18);

implementing individual diffusion rates for separate chemical species; the influence of the context of the larger hydraulic network on local leaching; and further refining the microstructure model of the cement. Apart from validation from experiments reported in the literature, the next step for validation is to model the leaching of real pipes that have been in use for several decades, based on several historic and recent condition measurements with phenolphthalein. Given the substantial sensitivity of the system to the initial porosity of cement, lab experiments probing the microstructure of actual pipe material would be preferable to provide the best model input assumptions.

After these refinement, the next research step is to use the model to carry out an extensive sensitivity analysis to start searching for the water compositions that optimally protect against leaching, and to find out how well the effectiveness of compositions can be gauged from the various existing index parameters.
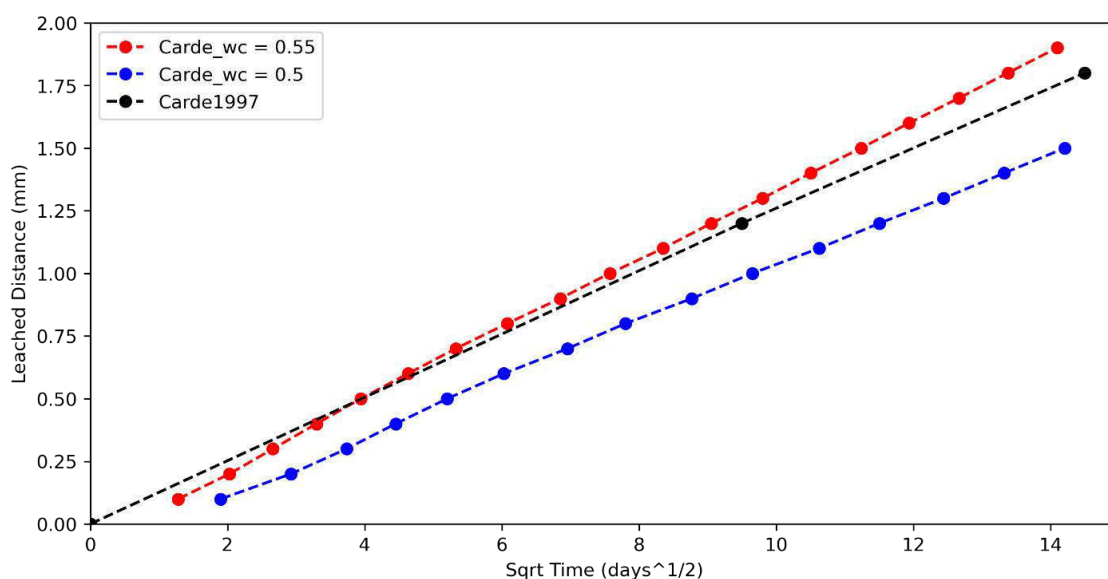

Figure 5. Comparison of the model outcomes to the experiments reported by 0. The red and blue curves indicate the modelled progression over time of the leached dept. The black markers indicate the reported leached depths during the experiments.

5 ACKNOWLEDGEMENTS

6 REFERENCES

[1] P. Leroy, M.R. Schock, I. Wagner, and H. Holtschulte, Cement-based materials in Internal Corrosion of Water Distribution Systems, 1st ed., Denver: AWWA Research Foundation, 1996.

[2] J.R. Rossum and D.T. Merrill, An evaluation of the calcium carbonate saturation indexes, AWWA Journal, vol. 75, no. 2, February 1983, pp 95-100.

[3] P.J. de Moel, A.W.C. van der Helm, M. van Rijn, J.C. van Dijk, and W.G.J. van der Meer, Assessment of calculation methods for calcium carbonate saturation in drinking water for DIN 38404-10 compliance, Drinking Water Engineering and Science, vol. 6, November 2013, pp. 115-124.

[4] WHO, Guidelines for Drinking-water Quality, 4th ed., Geneva: WHO-Press, 2011.

[5] P. Torres-Lozada, K.A. Bueno-Zabala, L.G. Delgado-Cabrera, L.E. Barba-Ho, and C.H. Cruz-Velez, Corrosion control using hydroxide and bicarbonate alkalising agents in water drinking processes, Drinking Water Enginering and Science, vol. 8, March 2015, pp. 53-76.

[6] C. Carde, G. Escadeillas, and R. Francois, Use of ammonium nitrate solution to simulate and accelerate the leaching of cement pastes due to deionized water, Magazine of Concrete Research, vol. 49, no. 181, December 1997, pp.295-301.

[7] Jacques, D., Benchmarking of the Cement Model and Detrimental Chemical Reactions Including Temperature Dependent Parameters : Project Near Surface Disposal of Category A Waste at Dessel, report NIROND-TR 2009–30 E, Brussels: ONDRAF/NIRAS.

[8] C.A.J. Appelo, and D. Postma, D., Geochemistry, groundwater and pollution, 2nd ed., Leiden: Balkema Publishers, 2005.

[9] D.L. Parkhurst, and C.A.J. Appelo, Description of Input and Examples for PHREEQC Version 3 — A Computer Program for Speciation , Batch-Reaction , One-Dimensional Transport , and Inverse Geochemical Calculations. U.S., in Geological Survey Techniques and Methods, book 6, Florida: U.S. Geological Survey, 2013.

[10] B. Lothenbach, T. Matschei, G. Möschner, and F.P. Glasser, Thermodynamic modelling of the effect of temperature on the hydration and porosity of Portland cement. Cement and Concrete Research, vol. 38, no. 1, 2008, pp. 1–18.

[11] B. Lothenbach, and F. Winnefeld, Thermodynamic modelling of the hydration of Portland cement. Cement and Concrete Research, vol. 36, no. 2, 2006, pp. 209–226.

[12] S. Bejaoui, and B. Bary, B., Modeling of the link between microstructure and effective diffusivity of cement pastes using a simplified composite model. Cement and Concrete Research, vol. 37, no. 3, 2007, pp. 469–480.

[13] Eternit, Asbestcement Tabellen, product catalogus, Goor: Eternit, 1980.

[14] T. Powers, and T.L. Brownyard, Studies of the Physical Properties of Hardened Portland Cement Paste. ACI Journal Proceedings, vol. 43, no. 9, 1946.

[15] H.J.H. Brouwers, The work of Powers and Brownyard revisited: Part 1, Cement and Concrete Research, vol. 34, no. 9, 2004, pp. 1697–1716.

[16] R.A. Patel, J. Perko, D. Jacques, G. De Schutter, G. Ye, and K. Van Bruegel, Effective diffusivity of cement pastes from virtual microstructures: Role of gel porosity and capillary pore percolation, Construction and Building Materials, vol. 165, 2004, pp. 833–845.

[17] B.H. Oh, and S.Y. Jang, Prediction of diffusivity of concrete based on simple analytic equations. Cement and Concrete Research, vol. 34, 2004, pp. 463–480.

[18] A. Bentur, S. Mindess, and N. Banthia, N., The Interfacial Transition Zone in Fiber Reinforced Cement and Concrete State-of-the-Art Report of RILEM, In Engineering and Transport Properties of the Interfacial Transition Zone in Cementitious Composites.Paris: RILEM, 2004.

[19] E.J. Garboczi, and D.P. Bentz, Computer simulation of the diffusivity of cement-based materials. Journal of Materials Science, vol. 27, no. 8, 2004, pp. 2083–2092.

[20] Vitens, Vitens/phreeqpython: Object-oriented python wrapper for the VIPhreeqc module, https://github.com/Vitens/phreeqpython, May 2021.

[21] D. Jacques, J. Šimůnek, D. Mallants, J. Perko, and S.C. Seetharam, Evaluating changes of transport properties of chemically degrading concrete using a coupled reactive transport model, In 1st International Symposium on Cement-Based Materials for Nuclear Wastes, Avignon, France: Oct 2011.

[22] M. Moranville, S. Kamali, and E. Guillon, Physicochemical equilibria of cement-based materials in aggressive environments - Experiment and modelling, Cement and Concrete Research, vol. 34, no. 9, 2004, pp. 1569–1578.